Hindawi
Mathematical Problems in Engineering
Volume 2021, Article ID 5710894, 12 pages
https://doi.org/10.1155/2021/5710894

Research Article

An Analytical Solution for the Interaction of Waves with Arrays of Circular Cylinders

Zhao Mi,[1] Long Pengzhen,[1] Wang Piguang,[1] Zhang Chao,[2] and Du Xiuli[1]

[1]*College of Architecture and Civil Engineering, Beijing University of Technology, Beijing, China*
[2]*College of Civil Engineering, Fuzhou University, Fuzhou, China*

Correspondence should be addressed to Wang Piguang; wangpiguang1985@126.com

Received 9 June 2021; Accepted 29 September 2021; Published 11 October 2021

Academic Editor: Mathiyalagan Kalidass

This paper presents an analytical method to investigate the multiple scattering problem within arrays of vertical bottom-mounted circular cylinders subjected to linear incident waves. Based on the Laplace equation and boundary conditions on the seabed and surface, a formulation of a two-dimensional multiple scattering problem is first obtained by using the variable separation method. Furthermore, the analytical solution of the wave forces on multiple circular cylinders is derived, which consists of the incident wave force due to the linear incident wave and the scattered wave forces considering multiple scattering waves. The presented analytical solution is validated by comparing its results with a numerical method, and the result shows that the analytical solution is in good agreement with the numerical one. Finally, the multiple scattering analysis is conducted on arrays of cylinders with different incident wave numbers, distances between cylinders, and quantities.

1. Introduction

Many sea-crossing bridges and offshore structures have been built worldwide in recent years. Pile group foundations play an important role in these offshore structures, and ocean wave is one of the major loadings that threaten the safety of offshore structures. Therefore, it is necessary to determine the wave forces on offshore structures when designing and constructing those structures. Linear diffraction theory is often used to analyze the interaction of ocean waves with cylinders based on the potential theory. Based on this theory, an analytical solution for the linear wave diffraction by a bottom-fixed vertical circular cylinder in finite water depth was proposed by MacCamy and Fuchs [1]. This paper is to extend the analytical solution for a single circular cylinder to circular cylinder arrays.

Much attention has been paid to the wave forces on a single vertical cylinder. Morison et al. proposed the Morison equation to estimate the wave forces on slender cylinders, in which the force is composed of a drag force proportional to the square of the velocity and a virtual mass force proportional to the horizontal component of the accelerative force exerted on the mass of water displaced by the cylinder [2]. Except for a large circular cylinder, the diffraction wave theory was also used by researchers to obtain analytical solutions for wave-structure interaction problem of cylinders with various geometric shapes. Williams presented two different approximation methods to predict the wave forces on elliptical cylinders [3]. The first method is based on the exact expressions obtained by Chen and Mei [4], and the second is the integral equation method. Bhatta et al. presented an analytical approach to predict the wave forces due to scattering and radiation on a floating circular cylinder in the water of finite depth [5]. The inquiry into the interaction between a fixed vertical elliptical cylinder and short-crested waves was analyzed by Wang et al. [6]. Liu et al. presented analytical solutions to estimate the diffraction wave forces on a uniform vertical cylinder and a truncated cylinder whose cross sections are arbitrarily smooth [7, 8]. Zhai et al. investigated the diffraction of waves from a system that is made up of a cylinder and an arc-shaped wall and proposed an analytical solution using the eigenfunction expansion approach [9].

Except for a single cylinder, the wave-structure interaction of arrays of vertical structures subjected to incident

waves has drawn many scholars' attention because of the extensive applications of cylinder arrays in ocean engineering. Linton and Evans proposed an analytical solution, as an extension of the work of MacCamy and Fuchs, for linear wave diffraction on arrays of vertical circular cylinders [10]. The simplified approach was extended to the complementary radiation problem by Kim [11] and for application to incident focused wave groups on an array of circular cylinders by Walker and Taylor [12]. Other interactions between vertical cylinders and incident waves have been studied, such as a group of dual-cylinder systems with a thin and porous outer cylinder and an impermeable inner cylinder subjected to linear waves [13], arrays of elliptical cylinders wherein wave diffraction happened [14], an array of truncated cylinders with arbitrary cross section subjected to small steepness harmonic wave [15], and collections of vertical bottom-mounted cylinders with arbitrary cross section subjected to linear waves [16].

A few numerical schemes also have been proposed to investigate the wave-structure interaction. Ali et al. developed a finite difference numerical method to estimate wave forces on double vertical cylinders [17]. Wang et al. presented finite element solutions to compute the wave forces on arrays of vertical circular cylinders and circular inclined cylinders [18, 19]. Besides the finite element method (FEM), the scaled boundary finite element method (SBFEM) has been recently applied in studies on vertical cylinders with different cross-sectional shapes [20–22]. The SBFEM discretizes only the common interfaces of the subdomains with surface finite elements, and fully accurate results can be obtained by using only fewer elements.

In most analytical methods, the whole diffraction analysis mainly focused on the linear incident wave on cylinders and the scattered wave generated by every cylinder, say the first-order scattered wave [10]. Nevertheless, upon impinging on each other, the first-order scattered wave is scattered by the cylinder, and then the second scattered wave is generated. Higher-order scattered wave is also generated in this manner. The term order denotes the scattering times that an incident wave has encountered. Therefore, this study aims to propose an analytical solution to investigate how multiple scattering waves influence the wave-cylinder interaction.

2. Mathematical Formulation

There is situated a group of N ($N \geq 2$) vertical circular cylinders in water with depth h, as shown in Figure 1. Water is assumed to be irrotational, inviscid, and incompressible. The origin of the global Cartesian coordinate system (x, y, z) is located on the seabed level, and the z-axis is directed vertically upwards. The center of the ith cylinder at (x_i, y_i) with radius a_i is taken as the origin of a local polar coordinate system (r_i, θ_i), where θ_i is measured counterclockwise from the positive x-axis.

Figure 2 shows the relation between a global coordinate system and a local coordinate system of the ith cylinder, where the coordinates of Q in global Cartesian coordinate system satisfy the following equations:

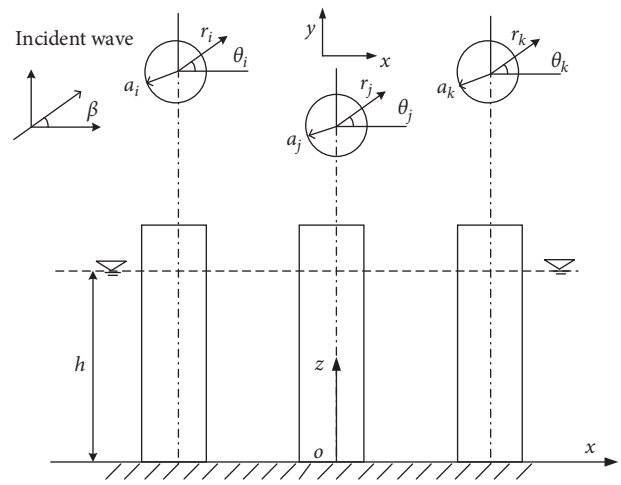

Figure 1: The interaction of water with arrays of circular cylinders.

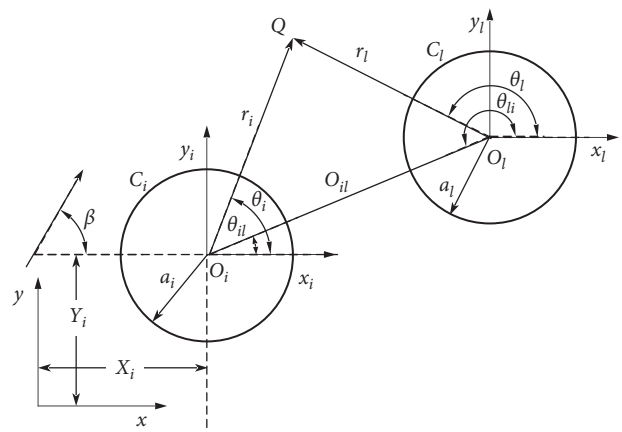

Figure 2: Coordinate systems and geometry for Graf's addition theorem adapted for multiple scattering problem.

$$x = X_i + x_i,$$
$$y = Y_i + y_i, \tag{1}$$

where X_i and Y_i are the coordinates of O_i of the local coordinate system of ith cylinder and (x_i, y_i) are the coordinates of Q in the local coordinate system of ith cylinder.

Assuming that the direction of wave propagation of an angle β to the positive x-axis and cylinders are exposed to the linear incident waves, the total wave pressure in the time domain can be written as $p^e = pe^{-i\omega t}$, with $i = \sqrt{-1}$, time t and the wave frequency ω, and the total wave pressure in the frequency domain p. The governing equation and boundary conditions are expressed in the polar coordinate system as

$$\frac{\partial^2 p}{\partial r^2} + \frac{1}{r}\frac{\partial p}{\partial r} + \frac{1}{r^2}\frac{\partial^2 p}{\partial \theta^2} + \frac{\partial^2 p}{\partial z^2} = 0. \tag{2}$$

(1) Seabed boundary condition ($z = 0$):

$$\frac{\partial p}{\partial z} = 0. \tag{3}$$

(2) The free surface condition ($z = h$):

$$-\frac{\omega^2}{g} p + \frac{\partial p}{\partial z} = 0. \tag{4}$$

(3) The Sommerfeld radiation conditions at infinity:

$$\lim_{r \longrightarrow \infty} \sqrt{r}\left(\frac{\partial p}{\partial r} - ikp\right) = 0, \tag{5}$$

where k satisfies the dispersion relation, which is expressed as $\omega^2 = gk \tanh kh$.

The total pressure p in the fluid domain consists of the incident wave pressure p^I and scattered wave pressure p^S, which satisfy the Laplace equation.

$$\nabla^2 p = \nabla^2 p^I = \nabla^2 p^S = 0. \tag{6}$$

3. Analytical Solution

In this part, as an isolated cylinder is exposed to the monochromatic incident waves, the interaction between it and the surrounding water will be reviewed first. Then, there will be an investigation on the multiple scattering problem among an array of circular cylinders, assuming that the influences on wave force of a column caused by other columns could be superposed approximately and the influence of column A on column B is immutable from other column.

3.1. Incident Wave Pressure. According to equation (6) and boundary conditions in equations (3) and (4), the incident wave pressure and the vertical mode of the fluid can be expressed as [23]

$$p^I = Z(z) e^{i\left(k_x x + k_y y\right)}, \tag{7}$$

$$Z(z) = \frac{\rho g H \cosh(kz)}{2 \cosh(kh)}, \tag{8}$$

in which $i = \sqrt{-1}$, ρ is the fluid density, H is the wave height, and k is the total wave number with $k_x = k \cos \beta$ and $k_y = k \sin \beta$.

The form of p_i^I in the corresponding local polar coordinate system of the ith cylinder (r_i, θ_i), also denoted by $p_i^{I,(0)}$, can be expressed as

$$p_i^{I,(0)} = \frac{\rho g H \cosh(kz)}{2 \cosh(kh)} \left[e^{iL_i k \cos\left(\psi_i - \beta\right)} \sum_{n=0}^{\infty} \beta_n J_n(kr_i) \cos n(\theta_i - \beta) \right], \tag{9}$$

where $\beta_n = \begin{cases} 1, & n = 0, \\ 2i^n, & n \geq 1 \end{cases}$ and J_n is the Bessel function of the first kind of order n.

3.2. First-Order Scattered Wave Pressure due to Incident Waves. The scattered wave pressure on the ith cylinder due to the linear incident waves is denoted by $p_i^{S,(1)}$ which is called the first-order scattered wave pressure. According to equation (7), after applying the variable separation method, $p_i^{S,(1)}$ can be expressed as

$$p_i^{S,(1)}(x, y, z) = P_i^{S,(1)}(x, y) Z(z). \tag{10}$$

Thus, the cylinder surface boundary condition for $P_i^{S,(1)}$ can be obtained as

$$\frac{\partial P_i^{S,(1)}}{\partial r_i}\Big|_{r_i = a_i} + \frac{\partial P_i^{I,(0)}}{\partial r_i}\Big|_{r_i = a_i} = 0. \tag{11}$$

Substituting equations (8) and (10) into equation (6), a two-dimensional Helmholtz equation in polar coordinate system is obtained as

$$\frac{\partial^2 P_i^{S,(1)}}{\partial r_i^2} + \frac{1}{r_i} \frac{\partial P_i^{S,(1)}}{\partial r_i} + \frac{1}{r_i^2} \frac{\partial^2 P_i^{S,(1)}}{\partial \theta_i^2} + k^2 P_i^{S,(1)} = 0. \tag{12}$$

Applying the variable separation method again, $P_i^{S,(1)}$ can be expressed as

$$P_i^{S,(1)}(r_i, \theta_i) = R(r_i) \Theta(\theta_i). \tag{13}$$

Substituting equation (13) into equation (12) yields the following equations:

$$\Theta'' + n^2 \Theta = 0, \tag{14}$$

$$r_i^2 R'' + r_i R' + \left(k^2 r_i^2 - n^2\right) R = 0. \tag{15}$$

The solution of equation (14) can be written as

$$\Theta_n(\theta_i) = A_{i,n}^{S,(1)} \cos n\theta_i + B_{i,n}^{S,(1)} \sin n\theta_i, \quad n = 0, 1, 2, \ldots. \tag{16}$$

According to the Sommerfeld radiation condition equation (5), the solution of equation (15) which is Hankel function is

$$R_n(r_i) = C_{i,n}^{S,(1)} H_n(kr_i), \tag{17}$$

where H_n is the Hankel function of the first kind of order n.

Hence, the solution of the scattered wave pressure $P_i^{S,(1)}$ can be expressed as

$$P_i^{S,(1)} = \sum_{n=0}^{\infty} H_n(kr_i) \left(E_{i,n}^{S,(1)} \cos n\theta_i + F_{i,n}^{S,(1)} \sin n\theta_i\right). \tag{18}$$

Substituting equations (18) and (9) into equation (11) and using the orthogonality of mode functions $\cos n\theta_i$ or $\sin n\theta_i$, $P_i^{S,(1)}$ can be obtained as

$$P_i^{S,(1)} = e^{ikL_i \cos\left(\psi_i - \beta\right)} \left[\sum_{n=0}^{\infty} -\frac{J_n'(ka_i)}{H_n'(ka_i)} \cos n\beta \, \beta_n H_n(kr_i) \cos n\theta_i + \sum_{n=0}^{\infty} -\frac{J_n'(ka_i)}{H_n'(ka_i)} \sin n\beta \, \beta_n H_n(kr_i) \sin n\theta_i \right]. \tag{19}$$

Figure 2 also shows geometric relations between two local polar coordinate systems. The first-order scattered wave pressure of other cylinder can be expressed in equation (19), but it is in its own local polar coordinate system. Thus, in order to calculate pressures in one coordinate, the Graf's addition theorem for Bessel functions can be recalled as [24]

$$\begin{aligned} H_n(kr_l)\cos n\theta_l &= \sum_{v=-\infty}^{\infty} H_{n+v}(kR_{il})J_v(kr_i)\cos\left[v\theta_i - n\pi - \overline{v+n}\theta_{il}\right], \\ H_n(kr_l)\sin n\theta_l &= -\sum_{v=-\infty}^{\infty} H_{n+v}(kR_{il})J_v(kr_i)\sin\left[v\theta_i - n\pi - \overline{v+n}\theta_{il}\right], \end{aligned} \tag{20}$$

where $R_{il} = \sqrt{(x_i - x_l)^2 + (y_i - y_l)^2}$.

Thus, with first-order scattered wave from the lth cylinder as the excitation source, the incoming wave impinging ith cylinder denoted by $P^{I,(1)}_{i\,\text{due to}\,P^{S,(1)}_l}$ can be expressed as

$$P^{I,(1)}_{i\text{due to}P^{S,(1)}_l} = \sum_{n=0}^{\infty} \frac{\beta_n J_n'(ka_l)}{H_n'(ka_l)} \begin{bmatrix} -\cos n\beta \sum_{v=-\infty}^{\infty} H_{n+v}(kR_{il})J_v(kr_i)\cos\left(v\theta_i - n\pi - \overline{v+n}\theta_{il}\right) \\ +\sin n\beta \sum_{v=-\infty}^{\infty} H_{n+v}(kR_{il})J_v(kr_i)\sin\left(v\theta_i - n\pi - \overline{v+n}\theta_{il}\right) \end{bmatrix} e^{ikL_l\cos(\psi_l - \beta)}. \tag{21}$$

Finally, the total incoming wave pressure on the ith cylinder due to the first-order scattered wave from other cylinders denoted by $P_i^{I,(1)}$ can be expressed as

$$P_i^{I,(1)} = \sum_{\substack{l=1 \\ l\neq i}}^{N} P^{I,(1)}_{i\text{due to}P^{S,(1)}_l}. \tag{22}$$

3.3. Higher-Order Scattered Wave Pressure. Higher-order scattered waves are generated in the same manner as mentioned in Section 3.2. For a general qth order scattered wave pressure on the ith cylinder denoted by $P_i^{S,(q)}$ $(q > 1)$, it can be obtained as

$$P_i^{S,(q)} = \sum_{n=0}^{\infty} H_n(kr_i)\left(E_{i,n}^{S,(q)}\cos n\theta_i + F_{i,n}^{S,(q)}\sin n\theta_i\right), \tag{23}$$

where the coefficients $E_{i,n}^{S,(q)}$ and $F_{i,n}^{S,(q)}$ can be obtained as

$$\begin{aligned} E_{i,n}^{S,(q)} &= -\frac{1}{\delta\pi kH_n'(ka_i)}\int_0^{2\pi}\frac{\partial P_i^{I,(q-1)}}{\partial r_i}\cos n\theta_i|_{r_i=a_i}\mathrm{d}\theta_i, \\ F_{i,n}^{S,(q)} &= -\frac{1}{\delta\pi kH_n'(ka_i)}\int_0^{2\pi}\frac{\partial P_i^{I,(q-1)}}{\partial r_i}\sin n\theta_i|_{r_i=a_i}\mathrm{d}\theta_i, \end{aligned} \tag{24}$$

where $\delta = 2$ if $n = 0$ or $\delta = 1$ if $n \neq 0$, and the superscript prime denotes the derivative to the Hankel function.

With $q-1$th order scattered wave from the lth cylinder as the excitation source, the incoming wave impinging ith cylinder denoted by $P^{I,(q-1)}_{i\text{due to}P^{S,(q-1)}_l}$ can be expressed as

$$\begin{aligned} P^{I,(q-1)}_{i\text{due to}P^{S,(q-1)}_l} = \sum_{n=0}^{\infty}\sum_{v=-\infty}^{\infty} H_{n+v}(kR_{il})J_v(kr_i) \\ \begin{bmatrix} E_{l,n}^{S,(q-1)}\cos\left(v\theta_i - n\pi - \overline{v+n}\theta_{il}\right) \\ -F_{l,n}^{S,(q-1)}\sin\left(v\theta_i - n\pi - \overline{v+n}\theta_{il}\right) \end{bmatrix}. \end{aligned} \tag{25}$$

The total incoming wave pressures on the ith cylinder due to the $q-1$th order scattered wave from other cylinders denoted by $P_i^{I,(q-1)}$ can be expressed as

$$P_i^{I,(q-1)} = \sum_{\substack{l=1 \\ l\neq i}}^{N} P^{I,(q-1)}_{i\text{due to}P^{S,(q-1)}_l}. \tag{26}$$

Substituting equation (26) into equation (24) and using the orthogonality, $E_{i,n}^{S,(q)}$ and $F_{i,n}^{S,(q)}$ can be simplified as

$$E_{i,n}^{S,(q)} = -\frac{1}{\delta H_n'(ka_i)}\sum_{\substack{l=1 \\ l\neq i}}^{N}\sum_{j=0}^{\infty}\frac{J_n'(ka_i)}{H_j'(ka_l)} \begin{Bmatrix} E_{l,j}^{S,(q-1)}\begin{bmatrix} H_{j+n}(kR_{il})\cos\left(j\pi + \overline{j+n}\theta_{il}\right) \\ +(-1)^n H_{j-n}(kR_{il})\cos\left(j\pi + \overline{j-n}\theta_{il}\right) \end{bmatrix} \\ +F_{l,j}^{S,(q-1)}\begin{bmatrix} H_{j+n}(kR_{il})\sin\left(j\pi + \overline{j+n}\theta_{il}\right) \\ +(-1)^n H_{j-n}(kR_{il})\sin\left(j\pi + \overline{j-n}\theta_{il}\right) \end{bmatrix} \end{Bmatrix},$$

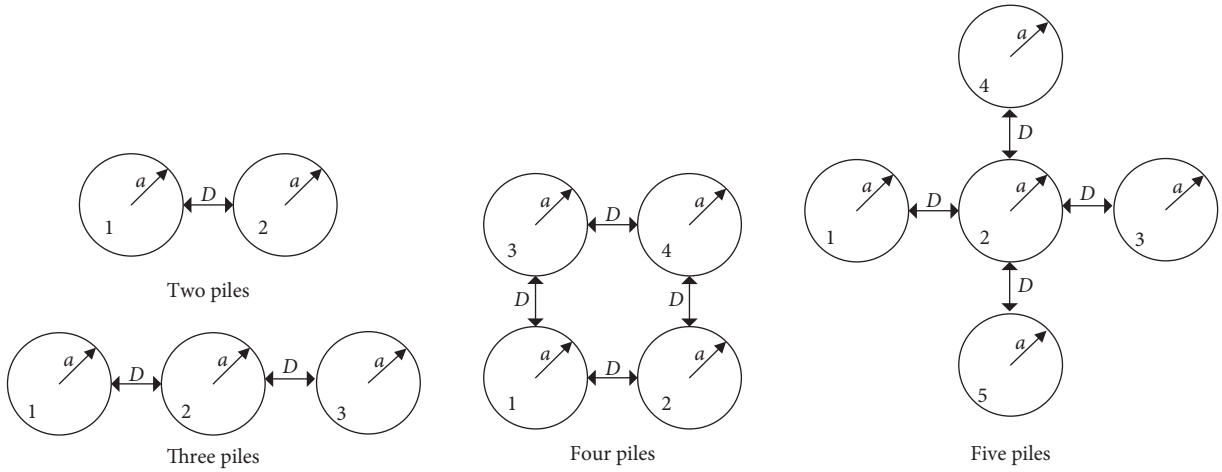

Figure 3: The sketch of pile group with N piles.

$$F_{i,n}^{S,(q)} = -\frac{1}{\delta H_n'(ka_i)} \sum_{\substack{l=1 \\ l\neq i}}^{N} \sum_{j=0}^{\infty} \frac{J_n'(ka_i)}{H_j'(ka_l)} \left\{ \begin{array}{l} E_{l,j}^{S,(q-1)} \begin{bmatrix} H_{j+n}(kR_{il})\sin\left(j\pi + \overline{j+n}\theta_{il}\right) \\ -(-1)^n H_{j-n}(kR_{il})\sin\left(j\pi + \overline{j-n}\theta_{il}\right) \end{bmatrix} \\ -F_{l,j}^{S,(q-1)} \begin{bmatrix} H_{j+n}(kR_{il})\cos\left(j\pi + \overline{j+n}\theta_{il}\right) \\ -(-1)^n H_{j-n}(kR_{il})\cos\left(j\pi + \overline{j-n}\theta_{il}\right) \end{bmatrix} \end{array} \right\}. \tag{27}$$

3.4. Wave Forces on the Cylinders. The wave pressure on the ith cylinder can be written as

$$P_i = \left[P_i^{I,(0)} + P_i^{S,(1)} + \sum_{q=2}^{\infty} \left(P_i^{S,(q)} + P_i^{I,(q-1)} \right) \right]. \tag{28}$$

Furthermore, the resultant circumferential wave force along x-axis and y-axis on the ith cylinder at height z is denoted by $f_i^x(z)e^{-i\omega t}$ and $f_i^y(z)e^{-i\omega t}$, where $f_i^x(z)$ and $f_i^y(z)$ are given by

$$f_i^x(z) = F_i^x \frac{\rho g H \cosh(kz)}{2\cosh(kh)}, \tag{29a}$$

$$f_i^y(z) = F_i^y \frac{\rho g H \cosh(kz)}{2\cosh(kh)}. \tag{29b}$$

According to the equation (28), F_i^x and F_i^y can be expressed as

$$F_i^x = -\int_0^{2\pi} P_i a_i \cos\theta_i \mathrm{d}\theta_i, \tag{30a}$$

$$F_i^y = -\int_0^{2\pi} P_i a_i \sin\theta_i \mathrm{d}\theta_i. \tag{30b}$$

Finally, the total wave force on the ith cylinder along the x-axis and y-axis can be calculated by

$$F_{i,x}^e = \int_0^h f_i^x(z)e^{-i\omega t}\mathrm{d}z, \tag{31a}$$

$$F_{i,y}^e = \int_0^h f_i^y(z)e^{-i\omega t}\mathrm{d}z. \tag{31b}$$

4. Numerical Results

As shown in Figure 3, four different configurations, two and three circular cylinders in tandem ($N = 2$, 3), four cylinders in square ($N = 4$), and five cylinders in cross star ($N = 5$), are used in this study to investigate the effect of higher-order scattered waves on wave forces, where D denotes the distance between two adjacent cylinders. A dimensionless parameter is defined as

$$D_r = \frac{D}{2a}, \tag{32}$$

where D denotes the distance between two adjacent cylinders and a denotes the radius of the cylinder.

4.1. Validation. The present analytical solution consists of an infinite series including all the scattering waves in any order, which shall be truncated into a finite term in computation since the calculation speed is limited by the number of the term. As shown in Figures 4 and 5, the results will converge when truncating the infinite series into 15–18 terms. Therefore, the truncation order is selected as $q = 15$ in the following analysis.

The case with $N = 2$ is firstly used to verify the effectiveness of the proposed analytical solution. Figure 6 shows the wave force F_i^x versus ka on two cylinders in tandem ($N = 2$) with $\beta = 0^\circ$, $\beta = 45^\circ$, and $\beta = 90^\circ$ of the present method and FEM [18]. The cases with $N = 3$, 4, and 5 are further used to verify the effectiveness of the proposed analytical solution. Figures 7 and 8 show the wave field (P) obtained by the present method and FEM, respectively. The

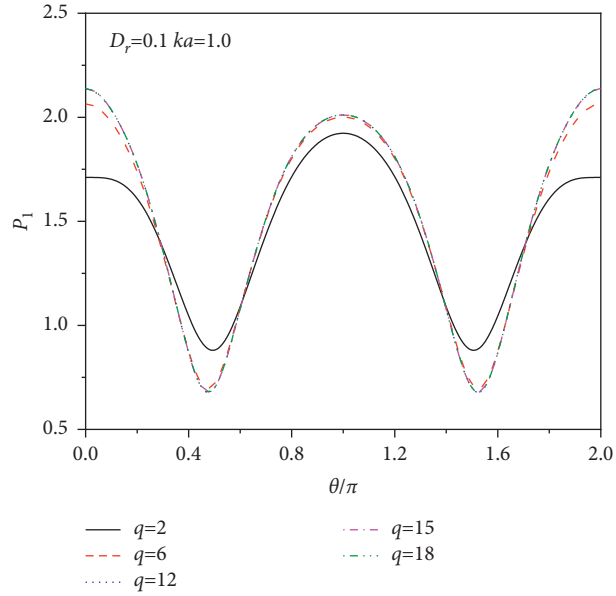

Figure 4: The wave pressures on the first cylinder P_1 versus θ for different q with $\beta = 0^\circ$ and $N = 2$.

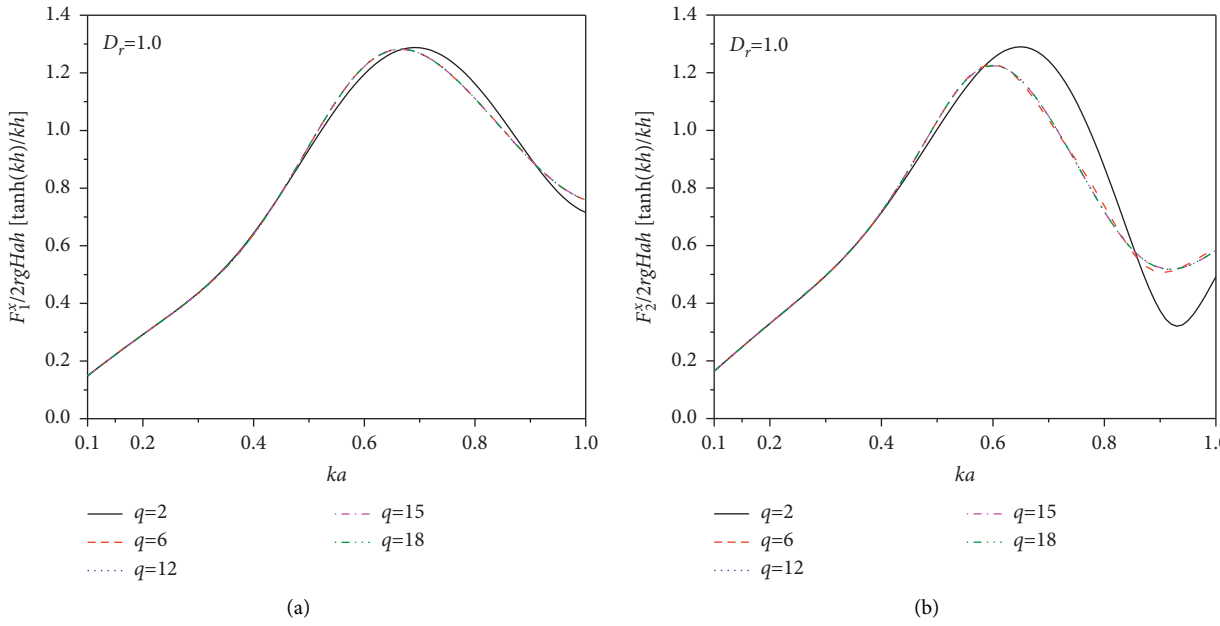

Figure 5: The wave forces F_i^x versus ka for different q with $\beta = 0^\circ$. (a) $N = 2$. (b) $N = 5$.

relative errors of wave pressure on each cylinder between Figures 7 and 8 are depicted in Figure 9. It can be concluded from Figures 6–9 that the present method agrees well with the FEM.

4.2. Effect of Higher-Order Scattered Waves. Two dimensionless parameters $I_i^x = F_{i,q=15}^x/F_{i,q=2}^x$ and $I_i^y = F_{i,q=15}^y/F_{i,q=2}^y$ are defined to investigate the effect of higher-order scattered waves on the wave forces on the cylinders, where $F_{i,q=2}^x$ and $F_{i,q=15}^x$ denote the total wave forces on the ith cylinder along the x-axis with $q = 2$ and $q = 15$, respectively; $F_{i,q=2}^y$ and $F_{i,q=15}^y$ denote the total wave forces on the ith cylinder along the y-axis.

The case with three cylinders arranged in tandem is investigated firstly. Figure 10 shows the ratios I_i^x and I_i^y versus ka with $D_r = 1$ for different β. Figure 11 shows the ratios I_i^x and I_i^y versus D_r with $\beta = 45^\circ$ for different ka. The effect of higher-order scattered waves on the wave forces on each cylinder along the x-axis decreases as the wave

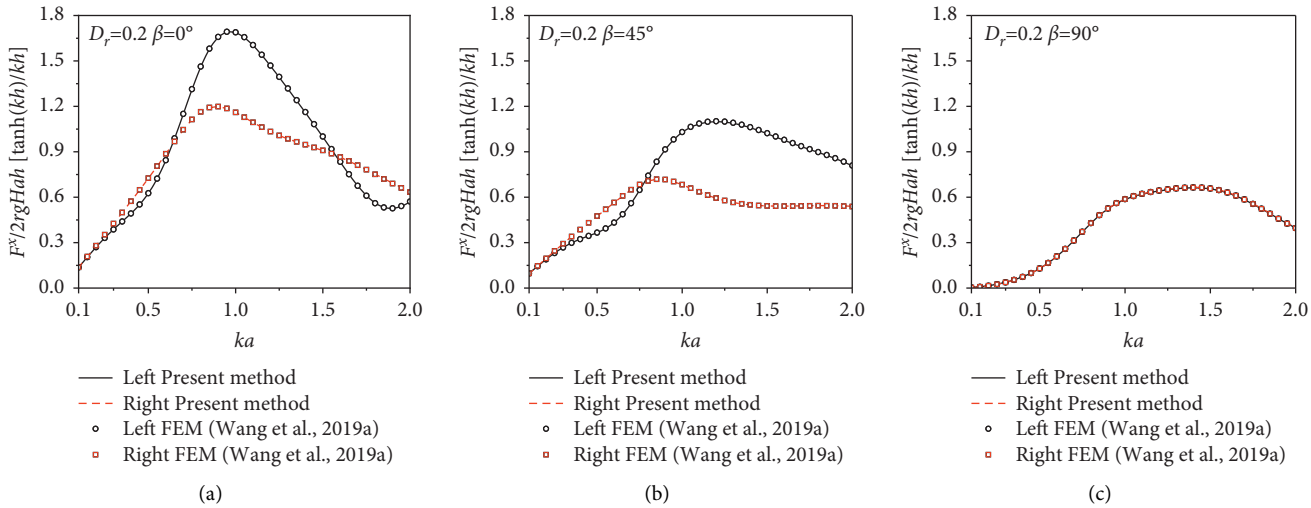

Figure 6: The wave forces on cylinders F_i^x versus ka with $N = 2$ obtained by the present method and the FEM [6]. (a) $\beta = 0^\circ$. (b) $\beta = 45^\circ$. (c) $\beta = 90^\circ$.

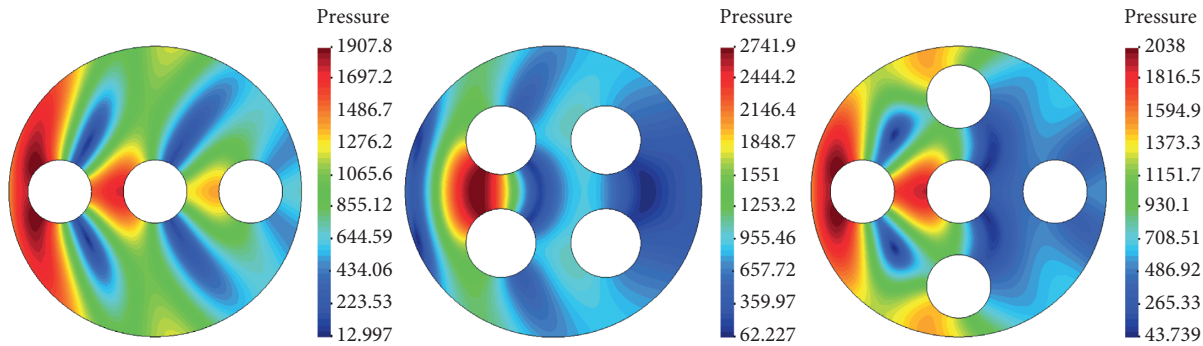

Figure 7: The wave field obtained by the present method with $ka = 1$, $D_r = 0.5$, and $a = 5$ m.

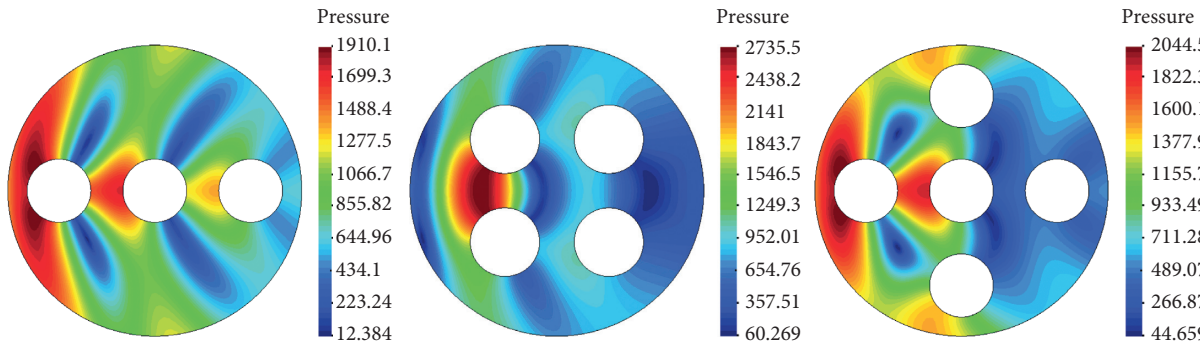

Figure 8: The wave field obtained by the FEM with $ka = 1$, $D_r = 0.5$, and $a = 5$ m.

propagation angle changes from $\beta = 0^\circ$ to $\beta = 60^\circ$. However, higher-order scattered waves have a limited impact on the wave forces along the y-axis.

The case with four cylinders arranged in square and five cylinders arranged in cross star are investigated secondly. Note that the wave force on C_3 and C_4 of the four cylinders and on the C_5 of the five cylinders is omitted due to the symmetry and wave propagation angle $\beta = 0^\circ$. It can be observed from Figures 12 and 13 that the effects of higher-order scattered waves on the wave forces on the cylinders can be ignored when ka is small (≤ 0.3), while the effects are significant when ka is large (>0.3). This means higher-order scattered waves can have more influence on the wave forces on the cylinders with larger wave number. The results also

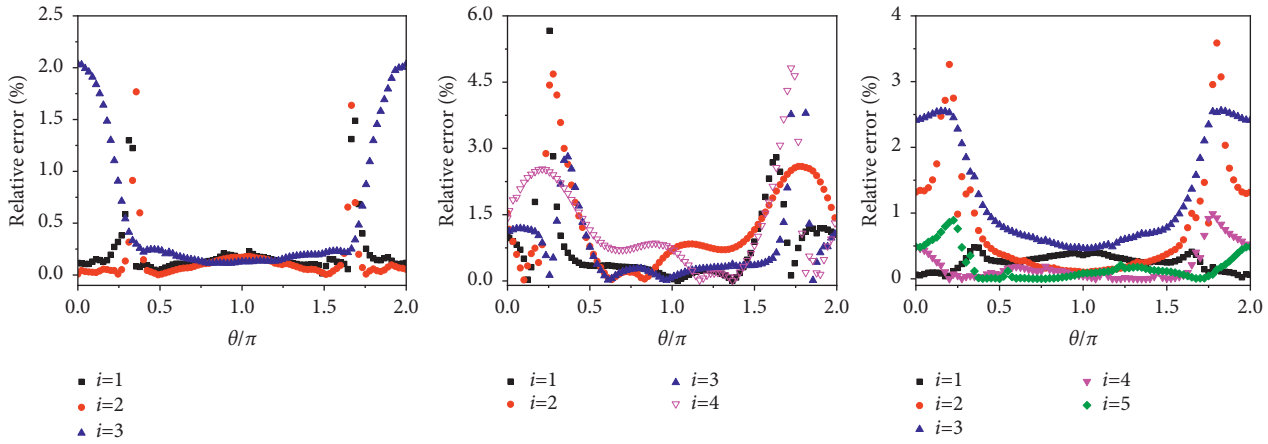

FIGURE 9: The relative error of the wave pressure between the present method and the FEM with $ka = 1$, $D_r = 0.5$, $a = 5$ m, and $N = 3, 4, 5$.

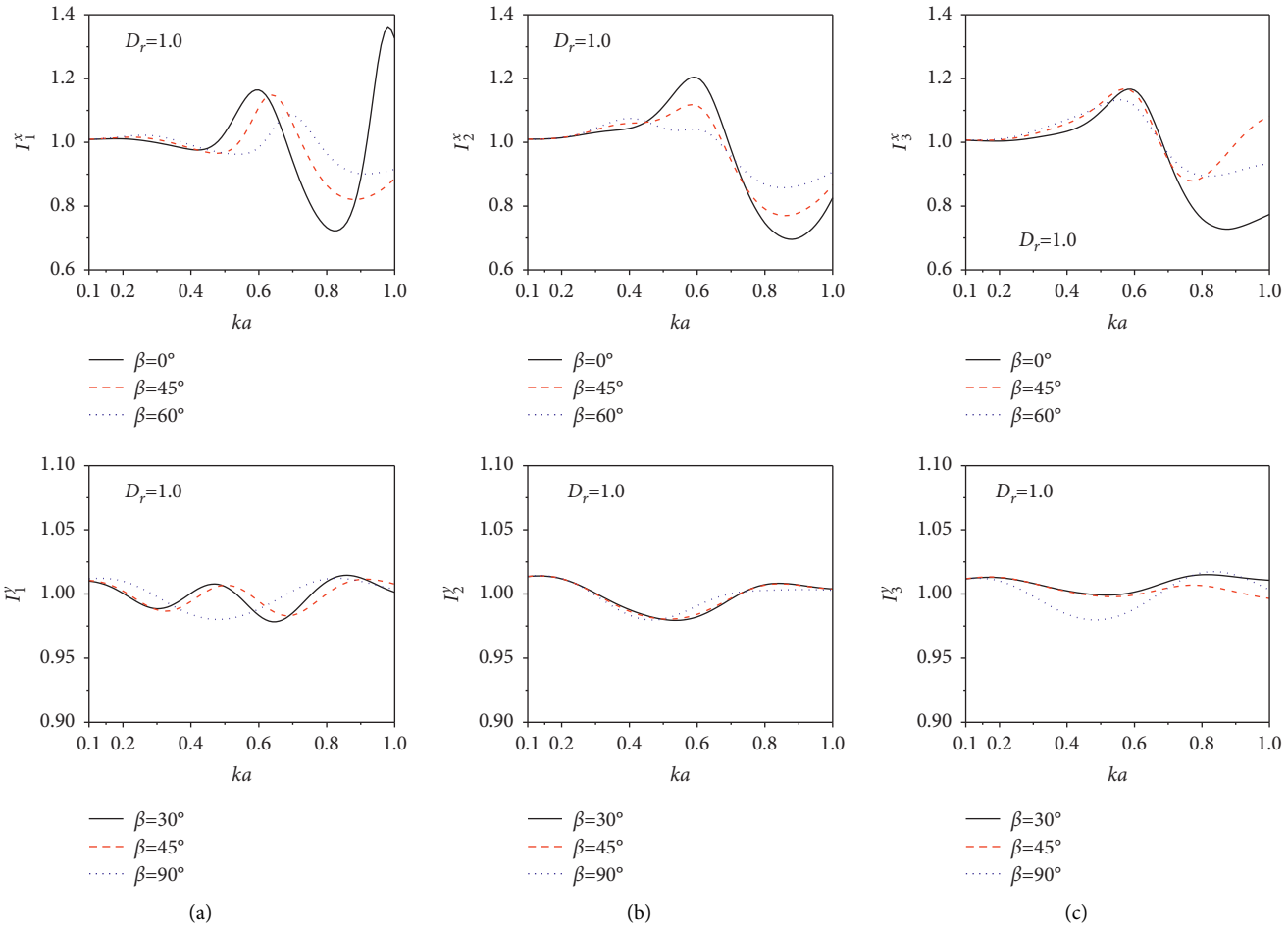

FIGURE 10: Ratios I_i^x and I_i^y versus ka for different β with $N = 3$. (a) Left pile. (b) Middle pile. (c) Right pile.

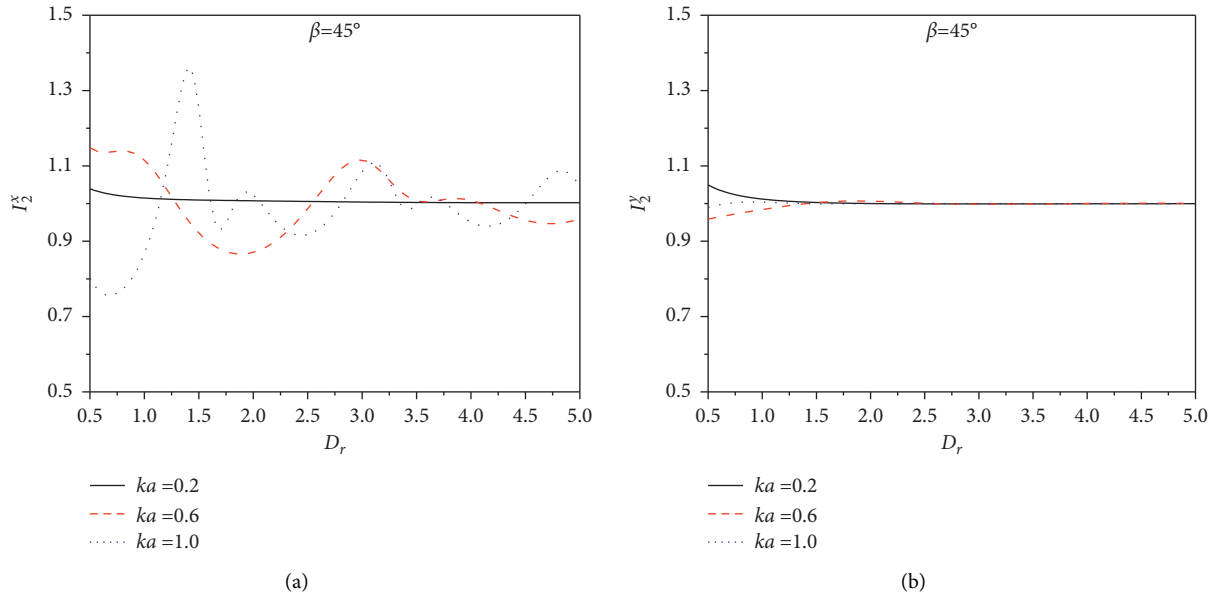

FIGURE 11: Ratios I_2^x and I_2^y of the middle pile versus D_r for different ka with $N = 3$. (a) I_2^x. (b) I_2^y.

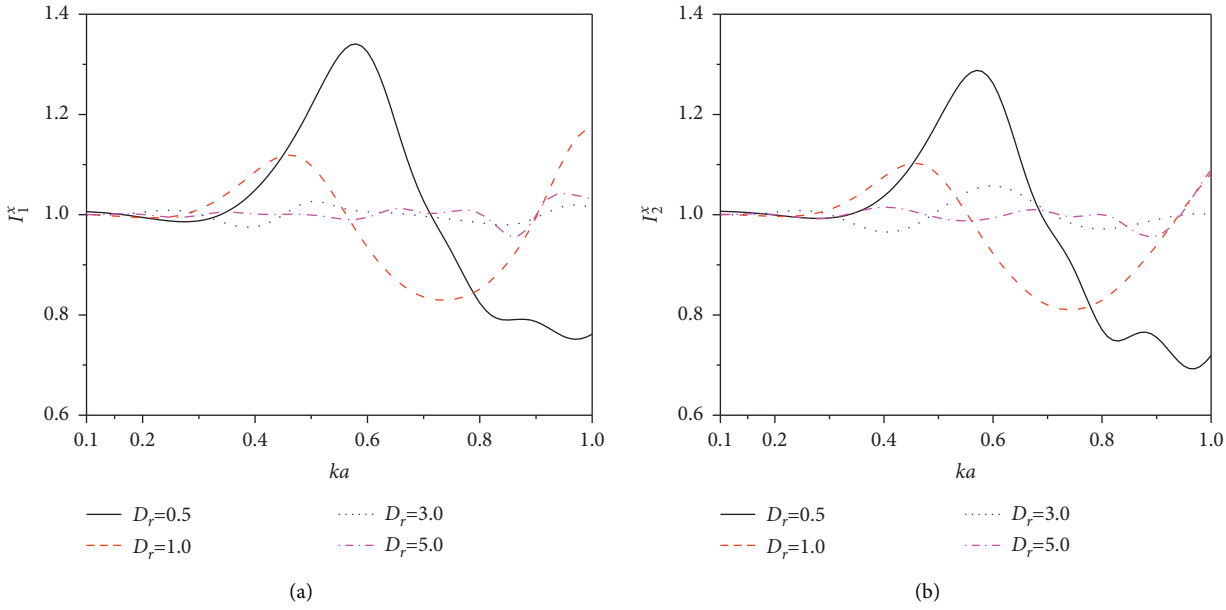

FIGURE 12: Ratio I_i^x versus ka for different D_r with $\beta = 0^\circ$ and $N = 4$. (a) Front pile. (b) Back pile.

indicate that the effect of higher-order scattered waves on the wave forces on the cylinders is significant when D_r is short between cylinders and that the influence tends to drop as the relative distance increases.

Figure 14 shows the ratio I_1^x of the first cylinder in all cases. It illustrates that the effect of higher-order scattered waves on the wave forces on the cylinder tends to increase as N increases.

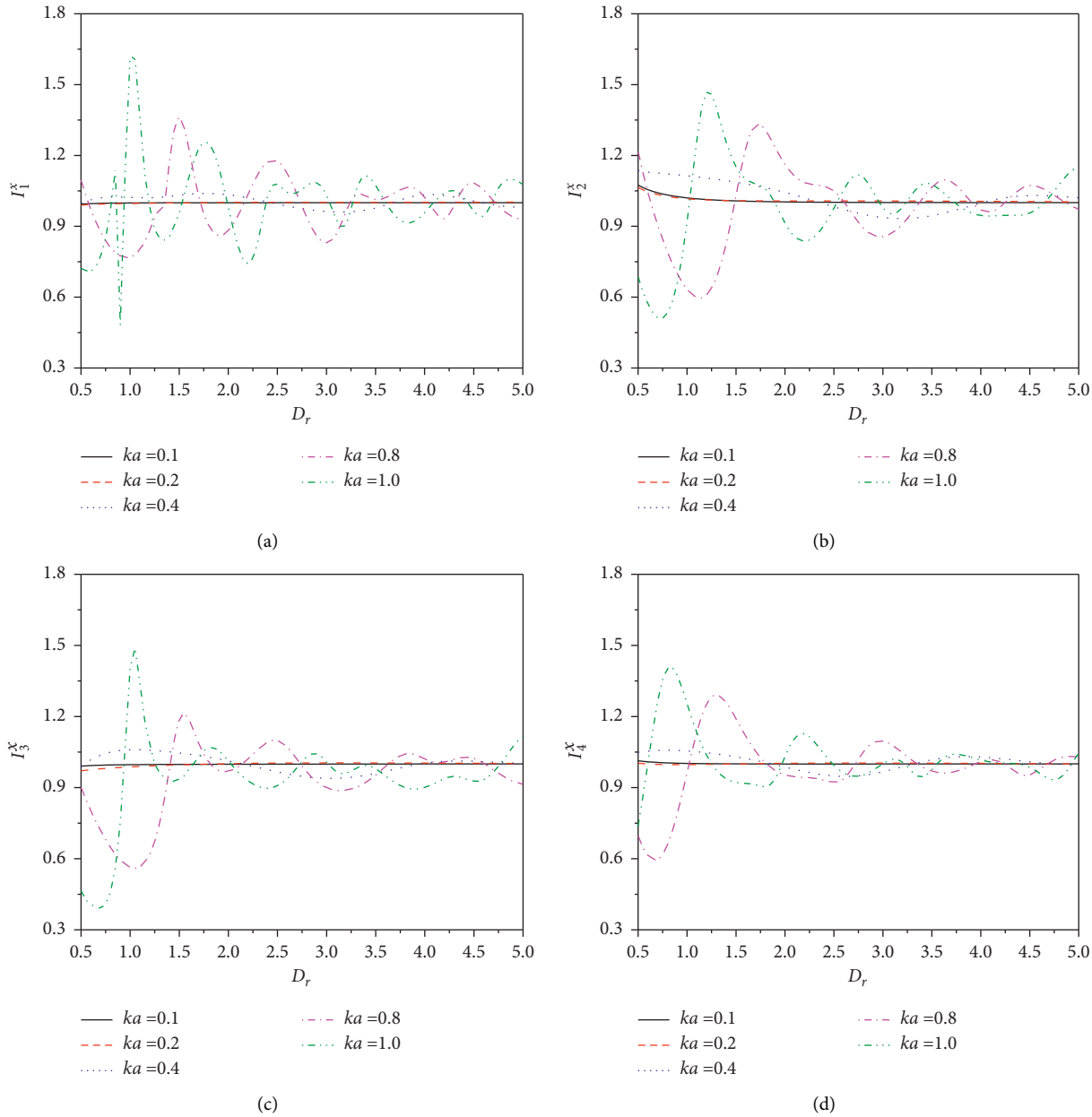

Figure 13: Ratio I_i^x versus D_r for different ka with $\beta = 0^\circ$ and $N = 5$. (a) Left pile. (b) Middle pile. (c) Right pile. (d) Top pile.

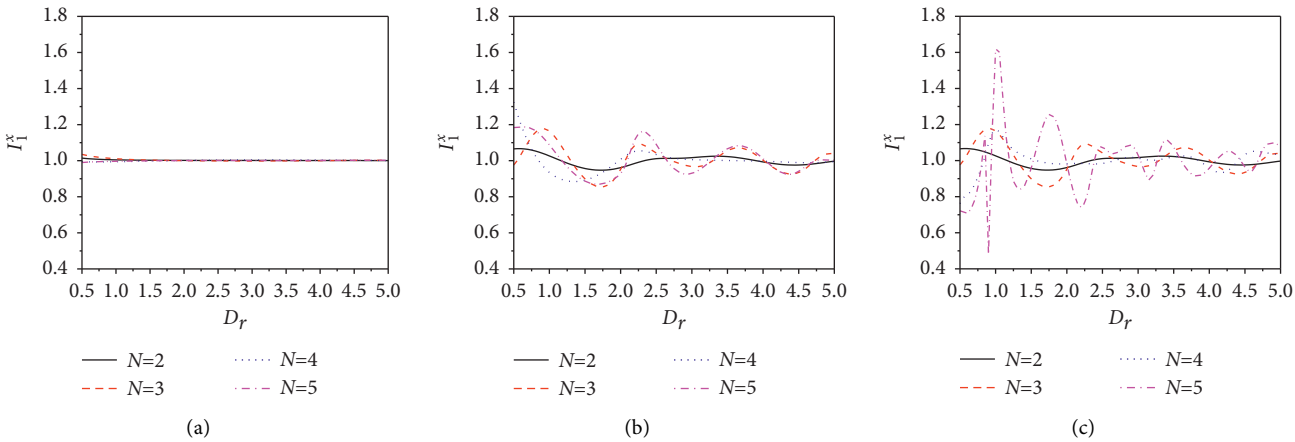

Figure 14: Ratio I_1^x of the first pile versus D_r with $\beta = 0^\circ$ and $N = 2, 3, 4, 5$. (a) $ka = 0.2$. (b) $ka = 0.6$. (c) $ka = 1.0$.

5. Conclusion

In this paper, an analytical method is presented to investigate wave forces on arrays of cylinders, which include the incident wave forces due to the linear incident waves, first-order scattered wave forces, and higher-order scattered wave forces due to lower-order scattered waves. The validation results indicate that the present analytical solution agrees well with the finite element method. The effect of higher-order scattered waves on the wave forces on the cylinders is investigated by using the proposed method. Based on the results, we can conclude that the effects of higher-order scattered waves on the wave forces on the cylinders tend to increase significantly as the wave number and the number of cylinders increase and as distance between cylinders decreases. When cylinders are arranged in tandem, the effects of higher-order scattered waves on the wave forces on cylinders along the x-axis decrease as the wave propagation angle increases, and the higher-order scattered waves have little influence on the wave forces on cylinders along the y-axis. It can also be concluded that the effects of higher-order scattered waves can be neglected when $ka \leq 0.3$.

Data Availability

No data were used to support this study.

Conflicts of Interest

The authors declare that there are no conflicts of interest regarding the publication of this paper.

Authors' Contributions

Zhao Mi and Wang Piguang were responsible for study concept and design. Long Pengzhen analyzed and interpreted the data and drafted the manuscript. Wang Piguang and Long Pengzhen were responsible for statistical analysis. Du Xiuli obtained funding and supervised the study. Zhao Mi, Wang Piguang, and Zhang Chao were responsible for critical revision of the manuscript for important intellectual content.

Acknowledgments

This study was jointly funded by the National Natural Science Foundation of China (52078010 and 51421005) and the Ministry of Education Innovation Team of China (IRT_17R03). Their financial support is gratefully acknowledged.

References

[1] R. C. MacCamy and R. A. Fuchs, *Wave Forces on Piles: A Diffraction Theory*, U.S. Beach Erosion Board, Washington, USA, 1954.

[2] J. R. Morison, J. W. Johnson, and S. A. Schaaf, "The force exerted by surface waves on piles," *Journal of Petroleum Technology*, vol. 2, no. 5, pp. 149–154, 1950.

[3] A. N. Williams, "Wave forces on an elliptic cylinder," *Journal of Waterway, Port, Coastal, and Ocean Engineering*, vol. 111, no. 2, pp. 433–449, 1985.

[4] H. S. Chen and C. C. Mei, "Wave forces on a stationary platform of elliptical shape," *Journal of Ship Research*, vol. 17, no. 2, pp. 61–71, 1973.

[5] D. D. Bhatta and M. Rahman, "On scattering and radiation problem for a cylinder in water of finite depth," *International Journal of Engineering Science*, vol. 41, no. 9, pp. 931–967, 2003.

[6] P. Wang, M. Zhao, X. Du, and J. Liu, "Analytical solution for the short-crested wave diffraction by an elliptical cylinder," *European Journal of Mechanics-B: Fluids*, vol. 74, pp. 399–409, 2019.

[7] J. Liu, A. Guo, and H. Li, "Analytical solution for the linear wave diffraction by a uniform vertical cylinder with an arbitrary smooth cross-section," *Ocean Engineering*, vol. 126, no. 1, pp. 163–175, 2016.

[8] J. Liu, A. Guo, Q. Fang, H. Li, H. Hu, and P. Liu, "Investigation of linear wave action around a truncated cylinder with non-circular cross section," *Journal of Marine Science and Technology*, vol. 23, no. 4, pp. 866–876, 2018.

[9] Z. Zhai, H. Huang, W. Ye, L. Yang, and S. Liu, "Hydrodynamic interactions between cnoidal waves and a concentric cylindrical structure with arc-shaped outer cylinder," *Ocean Engineering*, vol. 209, Article ID 107448, 2020.

[10] C. M. Linton and D. V. Evans, "The interaction of waves with arrays of vertical circular cylinders," *Journal of Fluid Mechanics*, vol. 215, no. -1, pp. 549–569, 1990.

[11] M. H. Kim, "Interaction of waves with N vertical circular cylinders," *Journal of Waterway, Port, Coastal, and Ocean Engineering*, vol. 119, no. 6, pp. 671–689, 1993.

[12] D. A. G. Walker and R. E. Taylor, "Wave diffraction from linear arrays of cylinders," *Ocean Engineering*, vol. 32, no. 17, pp. 2053–2078, 2005.

[13] K. Sankarbabu, S. A. Sannasiraj, and V. Sundar, "Interaction of regular waves with a group of dual porous circular cylinders," *Applied Ocean Research*, vol. 29, no. 4, pp. 180–190, 2007.

[14] I. K. Chatjigeorgiou and S. A. Mavrakos, "An analytical approach for the solution of the hydrodynamic diffraction by arrays of elliptical cylinders," *Applied Ocean Research*, vol. 32, no. 2, pp. 242–251, 2010.

[15] S. Zheng, Y. Zhang, J. Liu, and G. Iglesias, "Wave diffraction from multiple truncated cylinders of arbitrary cross sections," *Applied Mathematical Modelling*, vol. 77, pp. 1425–1445, 2020.

[16] J.-b. Liu, A.-x. Guo, Q.-h. Fang, H. Li, H. Hu, and P.-f. Liu, "Wave action by arrays of vertical cylinders with arbitrary smooth cross-section," *Journal of Hydrodynamics*, vol. 32, no. 1, pp. 70–81, 2020.

[17] L.-Y. M. Ali, M. S. Mehdi, and L.-Y. Amin, "Wave force on double cylindrical piles: a comparison between exact and finite difference solutions," *Journal of Marine Science and Application*, vol. 10, no. 1, pp. 33–40, 2011.

[18] P. Wang, M. Zhao, X. Du, and X. Cheng, "A finite element solution of earthquake-induced hydrodynamic forces and wave forces on multiple circular cylinders," *Ocean Engineering*, vol. 189, Article ID 106336, 2019.

[19] P. Wang, X. Wang, M. Zhao, X. Cheng, and X. Du, "A numerical model for earthquake-induced hydrodynamic forces and wave forces on inclined circular cylinder," *Ocean Engineering*, vol. 207, Article ID 107382, 2020.

[20] B. Li, L. Cheng, A. J. Deeks, and M. Zhao, "A semi-analytical solution method for two-dimensional Helmholtz equation," *Applied Ocean Research*, vol. 28, no. 3, pp. 193–207, 2006.
[21] X.-N. Meng and Z.-J. Zou, "Wave interaction with a uniform porous cylinder of arbitrary shape," *Ocean Engineering*, vol. 44, pp. 90–99, 2012.
[22] H. Song, L. Tao, and S. Chakrabarti, "Modelling of water wave interaction with multiple cylinders of arbitrary shape," *Journal of Computational Physics*, vol. 229, no. 5, pp. 1498–1513, 2010.
[23] C. M. Chiang, *The Applied Dynamics of Ocean Surface Waves*, World Scientific, Singapore, 1992.
[24] G. N. Watson, *Treaties of Theory of Bessel Functions*, Cambridge University Press, London, UK, 2nd edition, 1945.